Eur Biophys J (2004) 33: 238–246
DOI 10.1007/s00249-003-0355-2

ARTICLE

John Holyoake · Carmen Domene · Joanne N. Bright
Mark S. P. Sansom

KcsA closed and open: modelling and simulation studies

Received: 2 July 2003 / Accepted: 21 August 2003 / Published online: 22 October 2003

Abstract Bacterial homologues of mammalian potassium channels provide structures of two states of a gated K channel. Thus, the crystal structure of KcsA represents a closed state whilst that of MthK represents an open state. Using homology modelling and molecular dynamics simulations we have built a model of the transmembrane domain of KcsA in an open state and have compared its conformational stability with that of the same domain of KcsA in a closed state. Approximate Born energy calculations of monovalent cations within the two KcsA channel states suggest that the intracellular hydrophobic gate in the closed state provides a barrier of height $\sim 5\ kT$ to ion permeation, whilst in the open state the barrier is absent. Simulations (10 ns duration) in an octane slab (a simple membrane mimetic) suggest that closed- and open-state models are of comparable conformational stability, both exhibiting conformational drifts of ~3.3 Å Cα RMSD relative to the respective starting models. Substantial conformational fluctuations are observed in the intracellular gate region during both simulations (closed state and open state). In the simulation of open-state KcsA, rapid (< 5 ns) exit of all three K^+ ions occurs through the intracellular mouth of the channel. Helix kink and swivel motion is observed at the molecular hinge formed by residue G99 of the M2 helix. This motion is more substantial for the open- than for the closed-state model of the channel.

Presented at the Biophysical Society Meeting on Ion Channels – from structure to disease held in May 2003, Rennes, France

J. Holyoake · C. Domene · J. N. Bright · M. S. P. Sansom (✉)
Laboratory of Molecular Biophysics,
Department of Biochemistry,
University of Oxford,
South Parks Road, Oxford, OX1 3QU UK
E-mail: mark@biop.ox.ac.uk
Tel.: +44-1865-275371
Fax: +44-1865-275182

Present address: J. N. Bright
Research School of Chemistry,
The Australian National University,
0200 Canberra, ACT, Australia

Keywords Homology modelling · Ion channels · Molecular dynamics simulations · Potassium channels

Introduction

Ion channels are membrane proteins that enable rapid (i.e. near diffusion limited) yet selective passive flux of ions across biological membranes through a central pore surrounded by protein. The past few years have witnessed the determination of the structures of several species of ion channels, by X-ray diffraction (Bass et al. 2002; Chang et al. 1998; Doyle et al. 1998; Dutzler et al. 2002) and by cryoelectron microscopy (Miyazawa et al. 2003; Unwin 1993, 1995; Unwin et al. 2002). There have been substantial advances in structure determination of K channels, with X-ray structures having been determined for four different bacterial homologues of mammalian K channels. These are: (1) KcsA, a pH-gated K channel from *Streptomyces lividans* (Doyle et al. 1998; Zhou et al. 2001); (2) MthK, a Ca-gated K channel from *Methanobacterium thermoautotrophicum* (Jiang et al. 2002a); (3) KvAP, a voltage-gated K channel from *Aeropyrum pernix* (Jiang et al. 2003); and (4) KirBac, an inward rectifier K channel from *Burkholderia pseudomallei* (Kuo et al. 2003). Combined with a large body of functional and indirect structural data (reviewed by Yellen 2002), these structures provide an opportunity to relate atomic resolution structures of K channels to their diverse physiological functions. These functions include important roles of K channels in the physiology of both excitable (e.g. control of resting membrane potentials and of the depolarizing phase of action potentials) and non-excitable cells (e.g. regulation of insulin release from β-pancreatic cells) (Ashcroft 2000; Hille 2001).

All K channels have a common structural core, responsible for forming the central K^+-selective pore (Fig. 1). The channel is a tetramer, with each subunit contributing two transmembrane (TM) α-helices (called M1 and M2 in KcsA, MthK and KirBac; called S5 and S6 in Kv channels) plus a re-entrant loop [made up of a

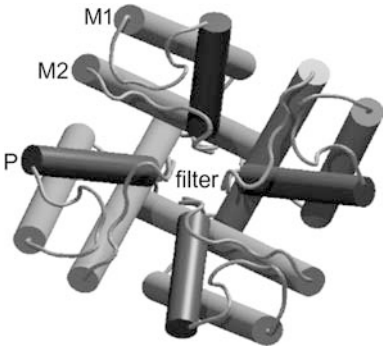

Fig. 1 Schematic diagram of the pore domain of a K channel, viewed from the extracellular mouth. The M1 and M2 helices are in *light grey*; the P helix in *dark grey*. This diagram is based on the closed-state structure of KcsA

P-helix and an extended filter (F) region]. The filter contains the TVGYG sequence motif that is characteristic of K channels. The eight TM helices, $(M1,M2)_4$, form an inverted truncated cone. The wider, extracellular end of the cone accommodates the $(P\text{-}F)_4$ region, with the backbone carbonyls of the filter directed inwards to form K^+ interaction sites. There are five interactions sites in the filter (S0 to S4, where S0 is at the extracellular mouth). Below site S4 is a water-filled cavity. In the crystal structure of KcsA this cavity binds a single, central K^+ ion, and is of sufficient volume to accommodate 25–30 water molecules.

The crystal structures of KcsA and KirBac correspond to closed conformations of the channel. The M2 helices are close together at the intracellular mouth of the channel, forming a narrow hydrophobic pore that presents an effective barrier to ion permeation. Site-directed spin-labelling studies of KcsA at low pH (under which conditions the channel opens) provided the first structural indication of how KcsA opened, via movement apart of the M2 helices to provide a wider intracellular mouth to the pore (Liu et al. 2001; Perozo et al. 1998, 1999). This model of gating was subsequently studied further by a variety of computational approaches (Allen and Chung 2001; Biggin and Sansom 2001; Mashl et al. 2001; Shen et al. 2002). A crystallographic insight into the nature of the open state of KcsA was provided by the structure of MthK. MthK is activated by Ca^{2+} ion binding to an intracellular domain, and the crystals were grown in the presence of Ca^{2+}, thus "locking" the protein in an open state. The homology of KcsA and MthK allowed a model for the open state of KcsA to be proposed (Jiang et al. 2002b). In this model the M2 helices are splayed apart via hinge bending at a conserved glycine residue (G99 in KcsA) so as to provide a wide intracellular mouth for the channel.

Molecular modelling and simulation provide a valuable tool for integration of structural data from disparate sources and for exploring the dynamic, functional implications of static (time- and space-averaged) crystal structures. A wide range of computational approaches have been used to explore the functional implications of the (closed-state) KcsA structure (as reviewed by e.g. Roux et al. 2000; Sansom et al. 2002), including molecular dynamics (MD) simulations (Allen et al. 1999, 2000; Bernèche and Roux 2000; Domene and Sansom 2003; Guidoni et al. 1999, 2000; Shrivastava and Sansom 2000, 2002; Shrivastava et al. 2002), continuum electrostatics calculations (Roux and MacKinnon 1999), Brownian dynamics simulations (Allen and Chung 2001; Corry et al. 2000; Mashl et al. 2001) and homology modelling studies intended to extrapolate from the KcsA structure to structures of mammalian homologues (Capener and Sansom 2002; Capener et al. 2000, 2002, 2003). Notable successes of these methods include estimation of the free energy landscape for ion permeation through the KcsA filter (Åqvist and Luzhkov 2000; Bernèche and Roux 2001) and prediction of the S0 K^+ ion interaction site from simulations based on the lower resolution KcsA structure, a site subsequently identified in the high resolution structure of the channel (Bernèche and Roux 2001; Sansom et al. 2002).

In this study we use homology modelling based on the structure of MthK to generate a candidate structure for the TM domain of KcsA in an open state. MD simulations of the closed-state and open-state KcsA structures are performed to compare the conformational stability of the two structures, and to explore the conformational dynamics of the ions, and of the protein in the filter and gate regions. The results support the proposal that the open state of KcsA is similar to that of MthK in the TM region, and also support the suggestion that G99 acts as a molecular hinge.

Methods

Molecular modelling

The coordinates of KcsA (1k4c) and MthK (1lnq) were taken from the RCSB (http://www.rcsb.org). Two models of the open state of KcsA were generated (Table 1). Model Open1 was a direct open-state homology model based on MthK; model Open2 was generated using the M1 and M2 helices of model Open1 plus the loops and filter from the (closed) KcsA crystal structure. The sequence alignment upon which these models were based was derived from that in Jiang et al. (2002b). Homology modelling was performed using Modeller v6 (http://guitar.rockefeller.edu/modeller/modeller.html). An ensemble of 100 models for each structure was

Table 1 Summary of simulations[a]

Simulation	Membrane	Atoms	Time (ns) restrained	Time (ns) unrestrained
Closed	Octane	49,289	0.2	10
Closed, lipid	POPC	40,376	0.2	>10
Open1	Octane	49,811	0.2	1^F+10
Open2	Octane	54,903	0.2	10

[a]Open1 = KcsA in open-state homology modelled on MthK; Open2 = KcsA in open-state modelled using M1 and M2 helices of Open1 plus loops and filter from the (closed) KcsA crystal structure;
[F]filter mainchain atoms restrained for 1 ns followed by 10 ns without any restraints

generated with fourfold symmetry restraints. Five models from each ensemble were selected on the basis of the best fit to the restraints and an assessment of stereochemical quality was also performed to select an overall best model (Morris et al. 1992). Interactive modelling was carried out using Quanta (Accelrys).

Ionization states for both models of KcsA were the same as in Domene and Sansom (2003), having been adjusted to match the results of pK_A calculations (Ranatunga et al. 2001). Thus, most of the sidechains remained in their default ionization states, but the sidechain of E71 was constructed in a protonated state to form a diacid hydrogen bond with the carboxylate group of D80. The N-termini were capped with acetyl groups and the C-termini with amide groups.

Simulations

In each case the simulation system consisted of the channel model embedded in an octane slab (Table 1). The latter has been shown (Capener and Sansom 2002; Guidoni et al. 1999, 2000; Tieleman and Sansom 2001; Tieleman et al. 2001) to act as a simplified model of a phospholipid bilayer that has a significantly lower viscosity and so enables substantial changes in helix packing on a nanosecond timescale, should such changes wish to occur (i.e. be energetically favourable). Octane is comparable in its dielectric properties to the core of a lipid bilayer (its dielectric constant is ~2) but has a viscosity that is orders of magnitude lower than that of a lipid bilayer. The octane slab was 25 Å thick. The protein/octane system was solvated with ~15,000 water molecules. For comparison, a simulation of the closed state of KcsA in a POPC bilayer (Domene and Sansom 2003) was also performed. In each simulation, three K^+ ions were placed within the channel, two in the filter (at sites S1 and S3) and one in the cavity.

Lipid parameters were based on those of Berger et al. (1997) and of Marrink et al. (1998). All MD stages were performed using GROMACS 3.0 using the default Gromacs forcefield. Parameters derived from those of Åqvist (1990) for use in GROMACS were used for the K^+ ions. The temperature of the system was maintained at 300 K using a Berendsen thermostat (Berendsen et al. 1984). The pressure was maintained at 1.0 bar using a Berendsen barostat and a compressibility of 5×10^{-5} bar^{-1}. The integration time step was 2 fs. Once the system was set up, an energy minimization was carried out followed by a 0.2 ns equilibration period where the protein and the cation positions were restrained. After this, unrestrained MD simulations were performed in the NPT (constant number of particles, pressure and temperature) ensemble. A cut-off was used for longer range interactions: 10 Å for van der Waals interactions and 18 Å for electrostatic interactions.

Results

Comparison of models

Before reporting the results of the simulations, it is informative to make a brief comparison of the two static models. Visualization (Fig. 2) of the pore linings of the two models reveals the main difference, namely the intracellular mouth of the pore. In the closed state of KcsA the intracellular mouth of the pore is constricted by a ring of hydrophobic V115 sidechains. In the open state the kink of the M2 helices at residue G99 results in a significantly wider pore in this region, such that there is complete continuity between the cavity and the aqueous phase on the intracellular side of the membrane.

This difference can be quantified by determining the pore radius profiles for the two models (Fig. 3A). For

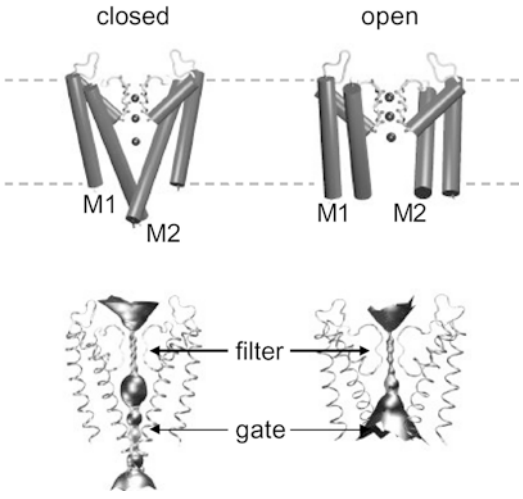

Fig. 2 Comparison of the closed- and open-state structures. The closed-state structure is shown on the *left-hand side* and an open-state model (model Open2: see Table 1) on the *right-hand side*. The *upper diagrams* show the helices (*cylinders*) and filter (*backbone atoms*) plus K^+ ions (*blue spheres*), along with the approximate position of the membrane (*horizontal broken lines*). The *lower diagrams* show the Cα trace plus the pore-lining surface [drawn using HOLE (Smart et al. 1996)]. In all cases, just two of the four subunits are shown (for clarity)

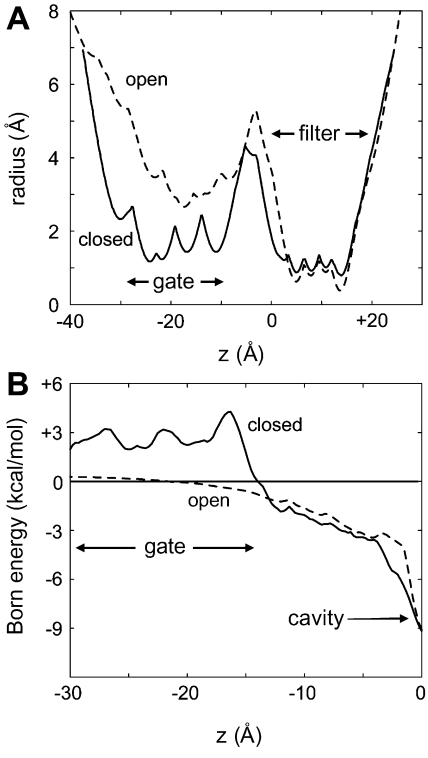

Fig. 3 **A** Pore radius profiles for the closed (*solid line*) and open (Open2, *broken line*) state structures. **B** Born energy profiles of the closed (*solid line*) and open (Open2, *broken line*) state structures in the vicinity of the intracellular gate

the closed-state model the minimum radius in the intracellular gate region is ~1.3 Å, i.e. the same as the radius of a (dehydrated) K^+ ion. Given the hydrophobic

nature of the pore lining in this region, this is expected to provide an effective barrier to ion permeation. In the open-state model the pore radius in the same region is ~3 Å. This is still a little less than the radius of a K^+ ion plus its first solvation shell (~4.3 Å), but taking into account random thermal fluctuations (see below) might be anticipated to present little if any barrier to ion permeation. In both models the radius in the filter region is substantially less than that of a dehydrated K^+ ion.

An *approximate* estimate of the effect of widening the intracellular pore on the energetics of ion permeation can be obtained by calculating the Born energy [i.e. the potential energy of solvation based on a simple continuum dielectric model of channel protein and of solvent (Daune 1999)] profile of a monovalent cation along the axis of the two pores (Fig. 3B). For the closed-state model the maximum barrier height is ~4.5 kcal/mol, i.e. $>7\ kT$. This would be expected to prevent *any* ion permeation in the absence of some change in conformation of the pore. In the open state the barrier has been completely removed.

We note that a smaller degree of expansion of the intracellular gate would have been sufficient to functionally open the pore. For example, both the EPR-derived model of Perozo and colleagues (Liu et al. 2001; Perozo et al. 1998, 1999) and the simulation-derived model of Biggin et al. (2001) proposed a smaller dilation of the intracellular mouth of the pore yet effectively remove most if not all of the Born energy barrier to ion permeation (data not shown).

Stability of simulations

Having established the functional difference between the static models, we compared their conformational stability via 10 ns MD simulations in a membrane-mimetic octane slab. Octane was used, rather than a full lipid bilayer, as it has a lower viscosity and thus would be expected to allow a greater degree of possible structural relation of a protein model on a 10 ns timescale. Based on our experience of simulations of other channels and membrane proteins, a 10 ns simulation in octane would be expected to be sufficient to reveal any (major) conformational instability of an open-state model.

A simple measure of the conformational stability of a membrane protein model is provided by the time-dependent root mean square deviation (RMSD) of the Cα atoms from their positions in the initial channel model. Comparison of Cα RMSDs for the Closed and Open2 simulations (Fig. 4) reveals an initial conformational drift to similar plateau values (~3.2 Å for Closed, ~3.4 Å for Open2) during the latter half of each simulation. For comparison, the Closed, lipid simulation gave a conformational drift of ~2.5 Å. Thus, we can see that the global conformational drift is somewhat higher in the octane slab environment than in the lipid bilayer environment, but does not differ significantly between the Closed and Open2 simulations.

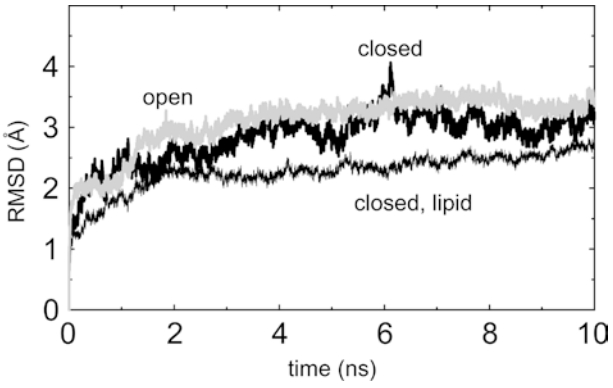

Fig. 4 Structural drift during the simulations. Cα RMSD relative to the starting model as a function of time for the Closed (*thick black line*), Closed, lipid (*thin black line*) and Open2 (*grey line*) simulations

Conformational fluctuations

In addition to the conformational drift, we may examine the magnitude of the fluctuations over the course of the simulation as a function of residue number (data not shown) and as a function of location of each residue (projected onto the pore, i.e. *z* axis; Fig. 5). The most

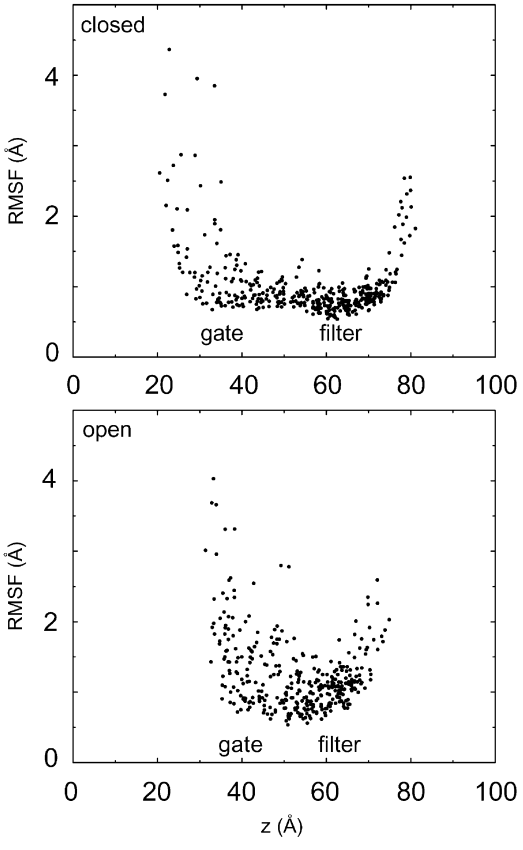

Fig. 5 Structural fluctuations as a function of residue position. Cα RMS fluctuations (vs. initial structure) as a function of the *z* position of the residue for the Closed (*upper*) and Open2 (*lower*) simulations

substantial fluctuations are in the ''turret'' loop between the M1 and P helices (for both the open and closed channels) and in the C-terminal half of M2 in the Open2 simulation. Projected onto the pore axis, the fluctuations can be seen to be highest in the intracellular gate region, in both the Closed and Open2 simulations. This supports observations in previous simulations of the closed state of KcsA (Bernèche and Roux 2000; Shrivastava and Sansom 2002) and suggests that this region may be ''primed'' for gating transitions. In both simulations the fluctuations are smallest in the filter region. There is some suggestion that the filter region fluctuations are a little greater in the Open2 simulation. This may reflect the distortion of the filter that occurs in the Open2 simulation subsequent to all three K^+ ions exiting the channel (see below).

K^+ ion trajectories

It is informative to compare the K^+ ion trajectories for the Closed and Open2 simulations (Fig. 6). In both cases the initial configuration of the system was with three K^+ ions within the channel, at sites S1 and S3 in the filter (with a water molecule in between at site S2) and at the site in the centre of the cavity. In the Closed simulation, similar behaviour to that observed in previous simulations of KcsA embedded in a POPC bilayer (Shrivastava and Sansom 2000, 2002) was observed. Thus, early on in the simulation (at ~0.3 ns) a concerted translocation of K^+-water-K^+ within the filter occurred, resulting in the two ions moving to sites S2 and S4. Following this transition, the two K^+ ions remain at sites S2 and S4 for the remainder of the simulation. At the same time, the ion within the cavity (K3 in Fig. 7A) initially moves a little deeper into the cavity and after remaining there for ~2 ns, spontaneously exits from the channel. Such exit of K^+ ions during Closed state KcsA simulations has been observed a number of times (Shrivastava and Sansom 2002) and is associated with a transient opening of the channel, along with transient hinge-bending distortion of the M2 helices.

The behaviour in the Open2 simulation is strikingly different. As in the Closed simulation there is an initial relaxation of the system during which K1-water-K2 translocates along the filter, leaving ions at sites S2 and S4. This appears to be coupled to an initial movement of K3 deeper into the cavity, followed very soon afterwards by its exit through the open intracellular gate. Thus it appears that in the open state of the channel there may be some degree of coupling between movements of ions along the filter and out of/into the cavity. In contrast to the closed-state simulation, in Open2 the two ions in the filter do not remain at sites S2 and S4, but instead exit the filter, in a semi-concerted fashion, after ~3 ns. Once K2 has left the filter, it does not remain in the cavity but instead exits the channel through the intracellular gate. This leaves just K1 at site S4. After a further ~0.3 ns it exits S4, sits just below S4 at the ''top'' of the cavity for ~1.5 ns, then rapidly leaves that channel through the open intracellular gate. Note that this leaves the filter devoid of ions from ~5 ns onwards (see below). Overall, these simulations suggest that, in the open state of the channel, an ion will not remain stably in the centre of the cavity but rather will rapidly exchange between the cavity and the intracellular solution.

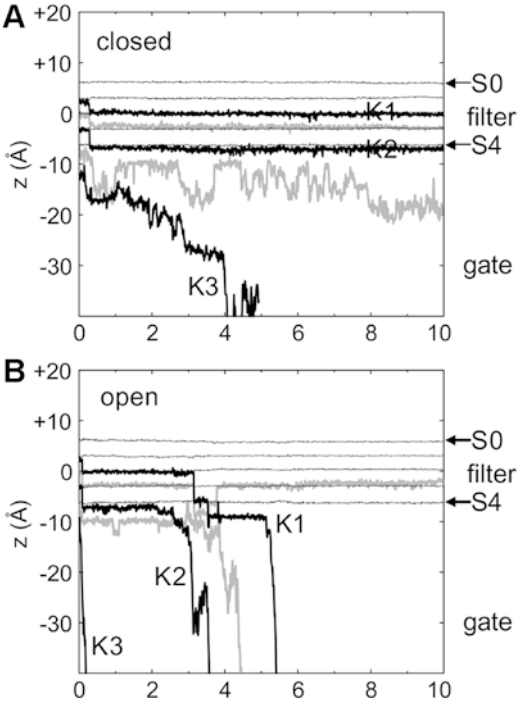

Fig. 6A, B Ion trajectories. Trajectories (projected onto the pore, i.e. *z*, axis) of the three K^+ ions (*thick black lines*) plus two intervening water molecules (*grey lines*), for the **A** Closed and **B** Open2 simulations. The *thin horizontal lines* indicate the positions of the filter interaction sites from S0 to S4. The approximate location of the gate is also indicated

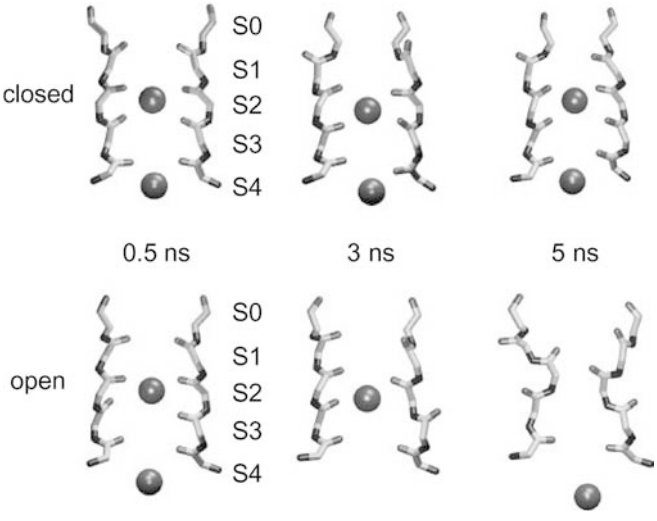

Fig. 7 Snapshots of the filter (*backbone atoms*, only two subunits for clarity) plus K^+ ions (*grey spheres*) at 0.5, 3 and 5 ns during the Closed and Open2 simulations

Conformational dynamics of the filter

Comparison of the conformational dynamics of the filter in the two simulations (Closed versus Open2) is interesting. As in previous closed-state simulations, the filter undergoes small conformation fluctuations during the course of the simulation. In particular, there are occasional "flips" of individual peptide carbonyls such that the oxygen atom points away from the filter (e.g. at 3 ns and 5 ns in Fig. 7). However, the overall conformation of the filter remains undistorted. The latter is true of the filter in the Open2 simulation whilst two K^+ ions remain within the filter. However, once both of the ions have exited the filter it undergoes a substantial distortion so as to considerably narrow the central section of the filter. Such a distortion has been seen in simulations of KcsA in the absence of any K^+ ions, and in simulations of a model of a mutant of Kir6.2 with altered conductance properties (Capener et al. 2003). It yields a filter conformation reminiscent of that observed in crystals of KcsA prepared in the presence of low K^+ ion concentrations (Zhou et al. 2001). In the absence of external K^+ ions in the Open2 simulation, we cannot say whether this conformational change would have been reversed upon entry of further ions into the filter.

Conformational dynamics of the gate

Analysis of the conformational dynamics of the gating helix (M2) in the closed and open simulations reveals some interesting differences. Visualization of superimposed snapshots from the Closed and Open2 simulations (Fig. 8) reveals a degree of flexibility of the M2 helix in both simulations, such that the intracellular ends of the M2 helices move relative to the remainder of the channel. This may be a little greater in the Open than the Closed simulations. However, neither simulation suggests a complete transition from one state to the other. This is perhaps not surprising, as one would envisage that such a transition would occur on a timescale longer than ~10 ns.

The conformational dynamics of the M2 helices can be examined rather more quantitatively in terms of the helix kink and swivel angle (Bright et al. 2002; Cordes et al. 2002), treating the conserved G99 as the hinge point. The results of this analysis (Fig. 9) confirm the difference in the conformation of M2 seen in the static models, such that for the Closed simulation the helix kink angle largely lies between 0° and ~20°. In contrast, for the Open simulation the average kink angle (over the last 2 ns of the simulation) is ~34°, but, more strikingly, M2 undergoes significantly larger fluctuations in kink and swivel than in the closed state. Furthermore, the kink and swivel angles are quite anisotropic, as has been seen in previous simulation of Kv channel S6 helices (Bright et al. 2002). Thus, these simulations confirm that G99 can indeed act as a molecular hinge. Interestingly, simulations of isolated M2 helices (Holyoake et al., unpublished data) also reveal hinge-bending motions, suggesting that this is an inherent property of the helix per se.

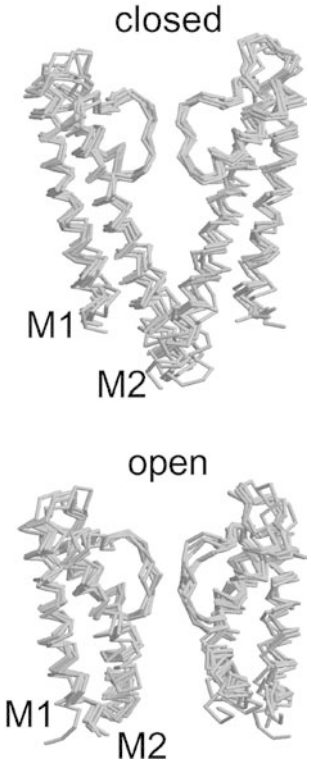

Fig. 8 Superimposed Cα traces (saved every 2 ns, 2 subunits only) from the Closed and Open2 simulations. The superimposition is on the Cα atoms of M1, P and the N-terminal half of M2

Discussion

These results are of relevance to our understanding of the gating mechanisms of K channels, and of ion channels in general. The simulation data strongly support the suggestion, based on comparison of X-ray structures of two different channels, that hinge bending of M2 in KcsA can result in a stable open state of the channel (Jiang et al. 2002b). In particular, they show that the open state of the channel presents no intracellular barrier to ion permeation, and that the M2 helices in the open state show conformational fluctuations about the M2 G99 residue which are consistent with the conformational change (i.e. hinge bending) proposed to underlie channel gating.

The hinge bending mechanism removes a substantial intracellular barrier to ion permeation formed by the ring of hydrophobic V115 residues. Based on the crystal structures of a number of channels, one may ask whether such a hydrophobic gate is likely to be a general feature of ion channels. As shown in Fig. 10, there are hydrophobic gates evident in the structures of KcsA, KirBac, nAChR and MscL, ranging in radius from 0.5 Å (KirBac) to 3.1 Å (nAChR). Simulation studies of

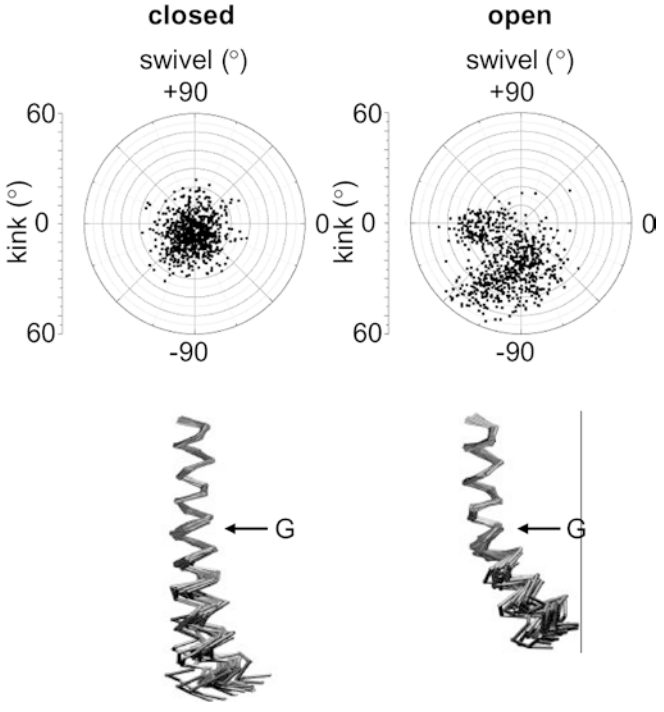

Fig. 9 M2 helix distortions: Closed and Open1 simulations compared. The *upper diagrams* show polar plots of the kink vs. swivel angle for M2 helix structures saved every 0.1 ns during the final 2 ns of each simulation for all four M2 helices. The *lower pair of diagrams* shows Cα traces of a single M2 helix, saved every 1 ns and superimposed on the Cα atoms of the N-terminal half of the helix. The position of the hinge-bending glycine residues (G) is labelled

a simple model of a hydrophobic gate in a transmembrane pore (Beckstein and Sansom 2003; Beckstein et al. 2001) reveal that a pore does not have to be physically occluded to form an energetic barrier to water (and thus by extension ion) permeation. Furthermore, channel opening can be achieved by either an increase in gate radius and/or an increase in polarity. Further simulations, based on a wider range of channel structures and models, should help to reveal whether such a mechanism is a general model for channel gating.

Critical evaluation of the methodology

There are a number of potential limitations in the methodology. The first is that of homology modelling the open structure of KcsA based on the structure of MthK. The first attempt (Open1) was a "direct" homology model. However, this proved problematic (and resulted in significant differences between model and template) in terms of the loops between the M1 and P helices, and between the filter and M2 helices. Thus, in model Open2 a more conservative strategy was adopted in which the closed-state structure of KcsA was used for the P helix, filter and loop regions, with the M1 and M2 helices homology modelled on the basis of the MthK structure. This had the advantage that the higher resolution KcsA structure was used for those regions that seemed to be unaltered in the lower resolution MthK. However, invariably some manual intervention was required to generate this model, and underlying it is the assumption that only the M1 and M2 helices change conformation significantly in going from the closed state. Of course, these issues could be resolved by a higher resolution structure of the MthK or, even better, KcsA open state.

The other main limitation from the modelling perspective is the absence of the N- and C-terminal intracellular domains from the KcsA structures. In the absence of any coordinates for these in either KcsA or MthK, it was not possible to do otherwise. The results of spin label studies (Cortes et al. 2001) have suggested a model for the C-terminal intracellular domain of KcsA. However, preliminary modelling and simulation studies (Capener 2002) suggest that this model of the C-terminal domain is rather unstable in 2 ns simulations of intact KcsA, and so further structural data are probably required. Both spin label data on KcsA (Cortes et al. 2001) and the structure of KirBac (Kuo et al. 2003) suggest that the region immediately N-terminal to M1 may form a short amphipathic helix that lies at the surface of the bilayer. It therefore may be possible to include this region in future models and simulations of KcsA.

From the simulation perspective the main possible limitation, as discussed in previous papers (Domene and Sansom 2003; Shrivastava et al. 2002) is the use of a (18 Å) cutoff rather than Ewald summation [which treats long-range interactions via an infinite array of periodic cells (Leach 2001)] to treat distant electrostatic interactions. As we have modelled the bilayer by an octane slab (thus omitting the charges on the lipid headgroups), the use of a cutoff is not likely to be the major approximation in the electrostatics. Furthermore,

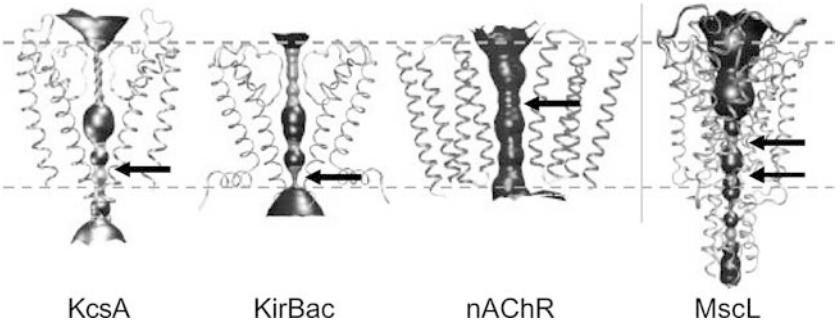

Fig. 10 Location of the hydrophobic gates in: KcsA (1k4c), KirBac (1p7b), nAChR (1oed) and MscL (1lnq). The pore-lining surface of each channel is indicated. The hydrophobic gates are indicated by the *arrows* and their radii and constituent sidechains are: KcsA, radius 1.3 Å, V115; KirBac, 0.5 Å, F146; nAChR, 3.1 Å, V255 and F256; and MscL, 1.7 Å, I14 and V21

recent work of Berkowitz (Bostick and Berkowitz 2003) has suggested that Ewald methods may result in artefacts (e.g. water orientational polarization) when applied to membrane proteins with a significant molecular dipole. For example, KcsA (which in our simulations has a net charge of +12) has a molecular dipole of ~190 Debye about the centre of the protein molecule, which might be anticipated to result in an interaction between KcsA and its replicas in adjacent periodic boxes. These issues need to be resolved and such effects examined in more detail.

Finally, the timescale of MD simulations is always open to question. The simulations in the current study (10 ns) are reasonable by current standards. The use of a (lower viscosity) octane slab rather than a full lipid bilayer may facilitate any likely conformation changes. However, we cannot exclude that significantly longer simulations might permit more substantial changes in, for example, the conformation and orientation of the M2 helices. Further studies are needed, on a variety of K channel models.

The more general relevance of this study is that it suggests how molecular modelling and simulation may be used to combine structural data from different sources to further explore possible gating models for ion channels. As further structures are determined, it will be increasingly important to use computational methods to aid the extrapolation from crystal structure to physiological function.

Acknowledgements We thank the Wellcome Trust and the BBSRC for funding, and the Oxford Supercomputing Centre for access to computing facilities. Our thanks to all of our colleagues for their interest in this work, and especially to Declan Doyle and to Nigel Unwin.

References

Allen TW, Chung SH (2001) Brownian dynamics study of an open-state KcsA potassium channel. Biochim Biophys Acta 1515:83–91

Allen TW, Kuyucak S, Chung SH (1999) Molecular dynamics study of the KcsA potassium channel. Biophys J 77:2502–2516

Allen TW, Bliznyuk A, Rendell AP, Kuyucak S, Chung SH (2000) The potassium channel: structure, selectivity and diffusion. J Chem Phys 112:8191–8204

Åqvist J (1990) Ion water interaction potentials derived from free-energy perturbation simulations. J Phys Chem 94:8021–8024

Åqvist J, Luzhkov V (2000) Ion permeation mechanism of the potassium channel. Nature 404:881–884

Ashcroft FM (2000) Ion channels and disease. Academic Press, San Diego

Bass RB, Strop P, Barclay M, Rees DC (2002) Crystal structure of *Escherichia coli* MscS, a voltage-modulated and mechanosensitive channel. Science 298:1582–1587

Beckstein O, Sansom MSP (2003) Liquid–vapor oscillations of water in hydrophobic nanopores. Proc Natl Acad Sci USA 100:7063–7068

Beckstein O, Biggin PC, Sansom MSP (2001) A hydrophobic gating mechanism for nanopores. J Phys Chem B 105:12902–12905

Berendsen HJC, Postma JPM, van Gunsteren WF, DiNola A, Haak JR (1984) Molecular dynamics with coupling to an external bath. J Chem Phys 81:3684–3690

Berger O, Edholm O, Jahnig F (1997) Molecular dynamics simulations of a fluid bilayer of dipalmitoylphosphatidycholine at full hydration, constant pressure and constant temperature. Biophys J 72:2002–2013

Bernèche S, Roux B (2000) Molecular dynamics of the KcsA K^+ channel in a bilayer membrane. Biophys J 78:2900–2917

Bernèche S, Roux B (2001) Energetics of ion conduction through the K^+ channel. Nature 414:73–77

Biggin PC, Sansom MSP (2001) Channel gating: twist to open. Curr Biol 11:R364–R366

Biggin PC, Shrivastava IH, Smith GR, Sansom MSP (2001) Non-equilibrium molecular dynamics study of KcsA gating. Biophys J 80:514

Bostick DL, Berkowitz ML (2003) The implementation of slab geometry for membrane-channel molecular dynamics simulations. Biophys J 85:97–107

Bright JN, Shrivastava IH, Cordes FS, Sansom MSP (2002) Conformational dynamics of helix S6 from Shaker potassium channel: simulation studies. Biopolymers 64:303–313

Capener CE (2002) Modelling and simulation studies of potassium channels, DPhil thesis, University of Oxford, p 223

Capener CE, Sansom MSP (2002) MD simulations of a K channel model: sensitivity to changes in ions, waters and membrane environment. J Phys Chem B 106:4543–4551

Capener CE, Shrivastava IH, Ranatunga KM, Forrest LR, Smith GR, Sansom MSP (2000) Homology modelling and molecular dynamics simulation studies of an inward rectifier potassium channel. Biophys J 78:2929–2942

Capener CE, Kim HJ, Arinaminpathy Y, Sansom MSP (2002) Ion channels: structural bioinformatics and modelling. Human Mol Genet 11:2425–2433

Capener CE, Proks P, Ashcroft FM, Sansom MSP (2003) Filter flexibility in a mammalian K channel: models and simulations of Kir6.2 mutants. Biophys J 84:2345–2356

Chang G, Spencer RH, Lee AT, Barclay MT, Rees DC (1998) Structure of the MscL homolog from *Mycobacterium tuberculosis*: a gated mechanosensitive ion channel. Science 282:2220–2226

Cordes FS, Bright JN, Sansom MSP (2002) Proline-induced distortions of transmembrane helices. J Mol Biol 323:951–960

Corry B, Kuyucak S, Chung SH (2000) Tests of continuum theories as models of ion channels. II. Poisson–Nernst Planck theory versus brownian dynamics. Biophys J 78:2364–2381

Cortes DM, Cuello LG, Perozo E (2001) Molecular architecture of full-length KcsA: role of cytoplasmic domains in ion permeation and activation gating. J Gen Physiol 117:165–180

Daune M (1999) Molecular biophysics: structures in motion. Oxford University Press, Oxford

Domene C, Sansom MSP (2003) A potassium channel, ions and water: simulation studies based on the high resolution X-ray structure of KcsA. Biophys J (in press)

Doyle DA, Cabral JM, Pfuetzner RA, Kuo A, Gulbis JM, Cohen SL, Cahit BT, MacKinnon R (1998) The structure of the potassium channel: molecular basis of K^+ conduction and selectivity. Science 280:69–77

Dutzler R, Campbell EB, Cadene M, Chait BT, MacKinnon R (2002) X-ray structure of a ClC chloride channel at 3.0 Å reveals the molecular basis of anion selectivity. Nature 415:287–294

Guidoni L, Torre V, Carloni P (1999) Potassium and sodium binding in the outer mouth of the K^+ channel. Biochemistry 38:8599–8604

Guidoni L, Torre V, Carloni P (2000) Water and potassium dynamics in the KcsA K^+ channel. FEBS Lett 477:37–42

Hille B (2001) Ionic channels of excitable membranes, 3rd edn. Sinauer, Sunderland, Mass

Jiang Y, Lee A, Chen J, Cadene M, Chait BT, MacKinnon R (2002a) Crystal structure and mechanism of a calcium-gated potassium channel. Nature 417:515–522

Jiang Y, Lee A, Chen J, Cadene M, Chait BT, MacKinnon R (2002b) The open pore conformation of potassium channels. Nature 417:523–526

Jiang Y, Lee A, Chen J, Ruta V, Cadene M, Chait BT, Mackinnon R (2003) X-ray structure of a voltage-dependent K^+ channel. Nature 423:33–41

Kuo A, Gulbis JM, Antcliff JF, Rahman T, Lowe ED, Zimmer J, Cuthbertson J, Ashcroft FM, Ezaki T, Doyle DA (2003) Crystal structure of the potassium channel KirBac1.1 in the closed state. Science 330:1921–1926

Leach AR (2001) Molecular modelling. Principles and applications, 2nd edn. Longman, Harlow, UK

Liu Y, Sompornpisut P, Perozo E (2001) Structure of the KcsA channel intracellular gate in the open state. Nat Struct Biol 8:883–887

Marrink SJ, Berger O, Tieleman DP, Jahnig F (1998) Adhesion forces of lipids in a phospholipid membrane studied by molecular dynamics simulations. Biophys J 74:931–943

Mashl RJ, Tang YZ, Schnitzer J, Jakobsson E (2001) Hierarchical approach to predicting permeation in ion channels. Biophys J 81:2473–2483

Miyazawa A, Fujiyoshi Y, Unwin N (2003) Structure and gating mechanism of the acetylcholine receptor pore. Nature 423:949–955

Morris AL, MacArthur MW, Hutchinson EG, Thornton JM (1992) Stereochemical quality of protein structure coordinates. Proteins Struct Funct Genet 12:345–364

Perozo E, Cortes DM, Cuello LG (1998) Three-dimensional architecture and gating mechanism of a K^+ channel studied by EPR spectroscopy. Nat Struct Biol 5:459–469

Perozo E, Cortes DM, Cuello LG (1999) Structural rearrangements underlying K^+-channel activation gating. Science 285:73–78

Ranatunga KM, Shrivastava IH, Smith GR, Sansom MSP (2001) Sidechain ionisation states in a potassium channel. Biophys J 80:1210–1219

Roux B, MacKinnon R (1999) The cavity and pore helices in the KcsA K^+ channel: electrostatic stabilization of monovalent cations. Science 285:100–102

Roux B, Bernèche S, Im W (2000) Ion channels, permeation and electrostatics: insight into the function of KcsA. Biochemistry 39:13295–13306

Sansom MSP, Shrivastava IH, Bright JN, Tate J, Capener CE, Biggin PC (2002) Potassium channels: structures, models, simulations. Biochim Biophys Acta 1565:294–307

Shen YF, Kong YF, Ma JP (2002) Intrinsic flexibility and gating mechanism of the potassium channel KcsA. Proc Natl Acad Sci USA 99:1949–1953

Shrivastava IH, Sansom MSP (2000) Simulations of ion permeation through a potassium channel: molecular dynamics of KcsA in a phospholipid bilayer. Biophys J 78:557–570

Shrivastava IH, Sansom MSP (2002) Molecular dynamics simulations and KcsA channel gating. Eur Biophys J 31:207–216

Shrivastava IH, Tieleman DP, Biggin PC, Sansom MSP (2002) K^+ vs. Na^+ ions in a K channel selectivity filter: a simulation study. Biophys J 83:633–645

Smart OS, Neduvelil JG, Wang X, Wallace BA, Sansom MSP (1996) Hole: a program for the analysis of the pore dimensions of ion channel structural models. J Mol Graph 14:354–360

Tieleman DP, Sansom MSP (2001) Molecular dynamics simulations of antimicrobial peptides: from membrane binding to trans-membrane channels. Int J Quantum Chem 83:166–179

Tieleman DP, Berendsen HJC, Sansom MSP (2001) Voltage-dependent insertion of alamethicin at phospholipid/water and octane/water interfaces. Biophys J 80:331–346

Unwin N (1993) Nicotinic acetylcholine receptor at 9 Å resolution. J Mol Biol 229:1101–1124

Unwin N (1995) Acetylcholine receptor channel imaged in the open state. Nature 373:37–43

Unwin N, Miyazawa A, Fujiyoshi Y (2002) Activation of the nicotinic acetylcholine receptor involves a switch in conformation of the α subunits. J Mol Biol 319:1165–1176

Yellen G (2002) The voltage-gated potassium channels and their relatives. Nature 419:35–42

Zhou Y, Morais-Cabral JH, Kaufman A, MacKinnon R (2001) Chemistry of ion coordination and hydration revealed by a K^+ channel-Fab complex at 2.0 Å resolution. Nature 414:43–48